Proceedings of AVEC '06
The 8th International Symposium on Advanced Vehicle Control, August 20-24, 2006, Taipei, Taiwan
AVEC060188

Safety Margin Estimation in Steady State Maneuvers

Matthijs Klomp[1] and Mathias Lidberg[2]
[1]Saab Automobile, [2]Chalmers University of Technology

Saab Automobile AB
A33-1 TICAG, 461 80 Trollhättan, SWEDEN
Phone: +46-520-84269
E-mail: matthijs.klomp@se.saab.com

This paper suggests a metric defining the margin of the actual longitudinal speed to a speed at which either the front or rear tires reach saturation. This margin is referred to as the safety margin of the vehicle. It is shown that this safety margin is particularly useful for systems that use continuous yaw-rate error elimination, such as advanced AWD systems. The proposed safety margin was evaluated using computer simulations.*

Topics / Vehicle Dynamics & Control, Driver Assistance Systems, Active Safety

1. INTRODUCTION

Advanced all-wheel drive (AWD) systems used in future fuel-cell and hybrid vehicle applications provide opportunities to control each wheel's torque individually. Front-wheel drive vehicles (FWD) tend to saturate the front wheels first since the maximum cornering force of the front tires is reduced when also used for driving. With the same argument rear-wheel drive vehicles (RWD) will tend to first saturate the rear wheels. AWD systems on the other hand are able to increase the cornering performance since the desired driving force can be distributed on all four wheels instead of only two [1]. The amount of driving force and how it is distributed on either front- or rear axle will addionally change the cornering behavior of the vehicle. FWD will increase the understeer of the vehicle and RWD will result in the vehicle to be oversteered at the limit.

An AWD system is assumed to then be controlled to anything between FWD or RWD. Torque vectoring, that is controlling the driving force between the left- and right wheels is a natural extension to the above.

Electronic stability control (ESC) systems used in current production vehicles use feedback control to eliminate the error between a reference and measured yaw rate [2] using individual braking to correct the vehicle motion. The ESC system is activated when the deviation between the reference and actual measured yaw rate is larger than a preset dead-band. In an ESC system a reference vehicle model using the steering signal as input is used to calculate the reference (desired) yaw-rate $\dot{\psi}^{ref}$. The reference vehicle model in the control system is based on linear tire characteristics and will deviate from the actual vehicle state when driven in the non-linear region of the tires. Driving in the non-linear region of the vehicle requires the driver to compensate the deviation from the desired path by use of the steering control.

By controlling the distribution of drive force using an AWD system the yaw-rate error can be continuously eliminated (within the limits of pure FWD or RWD). Since the yaw-rate error trigged the ESC system, the ESC system's intervention would be delayed by this continuous elimination. Additionally, and important to note, since the vehicle follows the path of the reference vehicle, the driver has a reduced feedback from the required steering input indicating that the tires are operating in the non-linear region.

It is therefore proposed to introduce a safety margin indicating the margin to a vehicle limit condition. This safety margin is required since the above discussion indicates the insufficiency of using the deviation from a reference as an indication of a limit condition.

The aim of this paper is to:

- Investigate and define the grip margin at the tire level.
- Relate tire limits to the vehicle limit conditions, that is; define a vehicle safety margin.
- Show the ability of proposed safety margin, using computer simulations, to detect the vehicle grip limits.

The vehicle safety margin is intended to be used for setting the boundaries between different control strategies which can be applicable depending on amount of margin available. Upon approaching the limit, the driver should be warned in such a way that the driver will take appropriate measures avoiding the need for utilizing the brake-system based stability control. The proposed vehicle safety margin should work independent of the control system is used to control the vehicle motion.

2. METHODOLOGY

Various ways of defining tire grip limits and vehicle safety limits are discussed in this paper and are evaluated using computer simulations using:

* The authors would like to thank the Swedish national research program "Intelligent Vehicle Safety Systems" for financial support.

- A vehicle model capturing the yaw-plane dynamics of an actual vehicle.
- A reference vehicle generating reference yaw-rate and lateral speed, used for feedback control.

In production vehicles equipped with ESC, the sensors available are steering wheel angle δ, yaw-rate $\dot{\psi}$ and lateral acceleration a_y but not the lateral speed v_y. Much research effort been put into reliably estimate the lateral speed [3], v_y which is here assumed to be known. The knowledge of the lateral speed is important for the calculation of tire slip angles as well as the estimation of the maximum available tire friction [4].

2.1. Vehicle Modeling

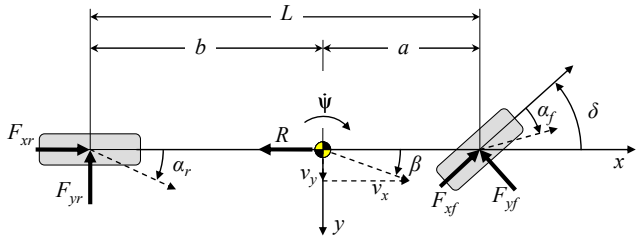

Figure 1. 3-DOF Bicycle Model

2.1.1. Model of Actual Vehicle

In order capture the main characteristics of an actual vehicle, only the planar motion of is considered. Since the roll and pitch dynamics have less influence in passenger vehicles they are in this case neglected [5]. Using the parameters defined in Figure (1) equations of motion are derived as:

$$m(\dot{v}_x - v_y\dot{\psi}) = F_{xf}\cos(\delta) - F_{yf}\sin(\delta) + F_{xr} - R \quad (1)$$

$$m(\dot{v}_y + v_x\dot{\psi}) = F_{xf}\sin(\delta) + F_{yf}\cos(\delta) + F_{yr} \quad (2)$$

$$I\ddot{\psi} = a(F_{xf}\sin(\delta) + F_{yf}\cos(\delta)) - bF_{yr} \quad (3)$$

Here R is the sum of all resistance forces imposed on the vehicle which, for the sake of simplicity are assumed to apply at the vehicle center of mass and only in the longitudinal direction:

$$R = \text{rolling} + \text{aero} + \text{grade} \quad (4)$$

The lateral and longitudinal forces, which are a result of both the vehicle states and vehicle input, are derived from a non-linear tire model described in detail in appendix A.

The normal forces required as input to calculate the tire forces are:

$$F_{zf} = (mgb - hm(\dot{v}_x - v_y\dot{\psi}))/L \quad (5)$$

$$F_{zr} = (mga + hm(\dot{v}_x - v_y\dot{\psi}))/L \quad (6)$$

2.1.2. Reference Vehicle Model

The vehicle model, used as reference for feedback control of the AWD and ESC system, has a fixed understeer gradient determined by linearized tire characteristics [2]. The model uses the steering angle as input and outputs the reference yaw-rate and lateral speed. Since the reference vehicle uses linear tire characteristics it will closely follow the actual vehicle on high-friction surface and moderate cornering. The actual vehicle will nevertheless deviate from the reference when driven in the non-linear tire-region.

The longitudinal speed v_x dependent 2-DOF vehicle model written on the form

$$\dot{r} = A(v_x)r + Bu \quad (7)$$

is derived from (1), (2) and (3) assuming a known constant v_x and linear tire characteristics where,

$$r = \begin{bmatrix} v^{\text{ref}} \\ \dot{\psi}^{\text{ref}} \end{bmatrix} \quad (8)$$

$$u = \delta \quad (9)$$

$$A = \begin{bmatrix} \frac{C_{\alpha f} + C_{\alpha r}}{mv_x} & \frac{aC_{\alpha f} - bC_{\alpha r}}{mv_x} - v_x \\ \frac{-aC_{\alpha f} + bC_{\alpha r}}{Iv_x} & \frac{-a^2C_{\alpha f} - b^2C_{\alpha r}}{Iv_x} \end{bmatrix} \quad (10)$$

$$B = \begin{bmatrix} \frac{C_{\alpha f} + F_{xf}}{m} \\ \frac{a(C_{\alpha f} + F_{xf})}{I} \end{bmatrix} \quad (11)$$

The lateral forces are assumed to be the product of the cornering stiffness of each axle, C_α, and the tire slip angle α:

$$F_y = C_\alpha\alpha = \left.\frac{\partial F_y}{\partial \alpha}\right|_{\alpha=0}\alpha \quad (12)$$

Each axle's respective slip angle is given from the kinematic relationships

$$\alpha_f = \delta - \arctan\left(\frac{a\dot{\psi} + v_y}{v_x}\right) \quad (13)$$

$$\alpha_r = \arctan\left(\frac{b\dot{\psi} - v_y}{v_x}\right) \quad (14)$$

, which together with (15) and the equations of motion result in the reference vehicle model.

3. VEHICLE LIMITS

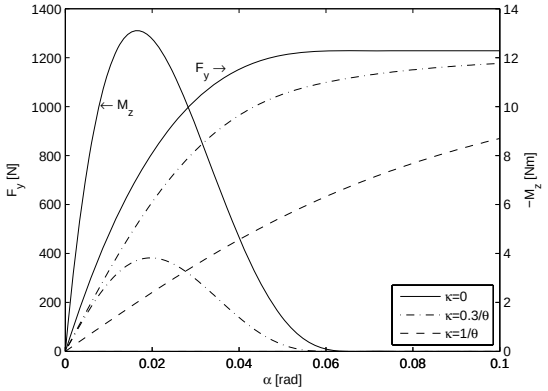

Figure 2. F_y and M_z at various levels of longitudinal slip, κ

3.1 Affect of AWD on Vehicle Behavior

For studying the safety limit, the behavior of the actual vehicle when approaching the grip limit is of interest. Before studying the vehicle limits, each axle is first studied individually. For the bicycle model the vehicle limits can be derived from the front and rear axle limits.

As can be seen from Figure (2), the cornering stiffness C_α and the lateral tire limits are affected by the amount of longitudinal force which is utilized, which is why the steering behavior is modified with drive-force distribution.

3.2. Vehicle Safety Margin

As mentioned in the introduction, a yaw-rate error independent vehicle safety margin is required. This vehicle safety margin captures the relationship between the vehicle states and the tire margin. Additionally the vehicle states expressed in limit states, such as a limit forward speed is intuitive.

The proposed vehicle safety margin is a simple relationship between the current- and a limit speed and is defined as:

$$\Lambda \triangleq \frac{v_x^{\lim} - v_x}{v_x^{\lim}} \tag{15}$$

Using the current understeer gradient ($K_u=\partial\delta/a_y$) to determine the limit speed $v_x^{\lim}$ not feasible since K_u could change sign when approaching the limit of the vehicle. Instead, $v_x^{\lim}$ is determined differently depending on which axle is the limiting one by checking the maximum yaw moment each axle can exhibit.

By checking if

$$M_{yf}^{\lim} < M_{yr}^{\lim} \tag{18}$$

, the front axle is the limiting factor if the above is true. If not, it is the rear axle that sets the limit. Are both equal, the vehicle is neutral. $M_y^{\lim}$ is defined as maximum possible yaw moment from each respective axle, given a certain longitudinal slip (κ) or longitudinal force F_x. Checking the above conditions will determine the limit understeer gradient $K_u^{\lim}$. The steady-state limit speed $v_x^{\lim}$ is now together with the current yaw-rate $\dot{\psi}$ determined from the steady-state solution to equations (2) and (3). In these equations the lateral force is replaced with $F_{yf}^{\lim}$ or $F_{yr}^{\lim}$, depending on which is the limiting axle. If of interest, the limit lateral speed can be similarly be derived from (1) and (3). This will result in the following solutions for the conditions mentioned above.

$$v_x^{\lim} = \frac{L(F_{yf}^{\lim} + F_{xf}\sin(\delta))}{bm\dot{\psi}} \quad ,\text{if } K_u^{\lim} > 0 \tag{19}$$

$$v_x^{\lim} = \frac{bF_{yr}^{\lim} - aF_{xf}\sin(\delta)}{am\dot{\psi}\cos(\delta)} \quad ,\text{if } K_u^{\lim} < 0 \tag{20}$$

$$v_x^{\lim} = \frac{\mu g}{\dot{\psi}} \quad ,\text{if } K_u^{\lim} = 0 \tag{21}$$

The tire limits $F_y^{\lim}$ assuming isotropic tire properties using the friction circle are:

$$F_y^{\lim} = \sqrt{(\mu F_z)^2 - F_x^2} \tag{22}$$

In the more common case with different friction in the longitudinal and lateral direction the limit lateral force $F_y^{\lim}$ becomes:

$$F_y^{\lim} = \mu_y F_z \sqrt{1 - \left(\frac{F_x}{\mu_x F_z}\right)^2} \tag{23}$$

3.3. Friction Estimation

The road friction μ is required as input for the vehicle safety estimation. In [4] a lateral grip margin ε using the self-aligning torque M_z from the tire to relate to the peak tire force is discussed. This ε ranges from 1→ 0, 1 being free-rolling and 0 having reached or exceeded the tire peak (μF_z). Additionally ε can be measured in a vehicle since it is related to the self-aligning torque (SAT) of the tire. The lateral grip margin based on the brush tire model is defined as:

$$\varepsilon \triangleq 1 - \frac{\sqrt{F_x^2 + F_y^2}}{\mu F_z} = 1 - \sigma\theta \triangleq \lambda, if\ \sigma \le \frac{1}{\theta} \tag{24}$$

In (24) σ is the combined wheel slip and θ a composite tire parameter discussed further in Appendix A.

Based on the fact that the self-aligning torque saturates prior to the lateral force, with the self aligning torque model rate defined as:

$$\gamma = \frac{M_z}{M_{z0}} \tag{25}$$

where

$$M_{z0} = \left(\frac{c}{6} + \frac{2c}{3}\frac{F_x}{C_\alpha}\right)F_y \tag{26}$$

and a way to relate the self aligning torque, the road surface friction could be estimated.

The relationship between self aligning torque model rate γ and the grip margin of the tires ε is shown in [6]

Since the self-aligning torque can be measured using direct or indirect measurement methods, this method of estimating the friction coefficient μ is proposed to be used in vehicle implementations of the vehicle safety margin.

4. EVALUATION

As previously discussed, vehicles with different drive force distribution will change the steering behavior of the vehicle. This is shown in Figure (3) where the steering angle is kept fixed and the vehicle speed is increased.

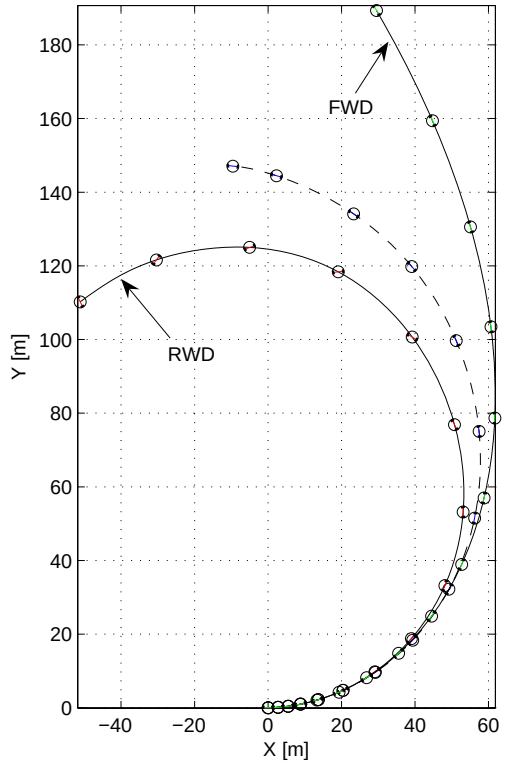

Figure 3. Vehicle trajectories at fixed δ and increasing v_x

4.1 Simulation of a Constant Radius Turn

In order to study the steady-state performance of three vehicle configurations (FWD, RWD and AWD), a standard constant radius cornering maneuver adapted from ISO 4138 was selected [8]. In the chosen maneuver, v_x is ramped from v_x = 20 → 65 km/h. The steering angle is changed as required for the vehicle will follow a constant radius R. The purpose of this maneuver is to show how the lateral grip margin, and not the yaw-rate or side-slip error is a good measure to describing a margin to the vehicle limit. The safety margin becomes especially useful if state-error elimination, using for instance an AWD system, is used prior to stability control. The simulation is performed with a fixed 5% longitudinal slip, κ, divided on either axle in the case of FWD and RWD and distributed throughout the maneuver in the case of AWD.

The steering angle required for a vehicle with a given understeer gradient to follow a circular path is given by the steady-sate relationship:

$$\delta = \frac{1}{R}\left(L + K_u \frac{v_x^2}{g} \right) \tag{16}$$

As can be seen from Figure (4), the required steering angle compared to the drivers' expectation (the reference vehicle) varies considerably between the three cases shown. For the AWD vehicle, the system is in this case controlled so its required steering angle to negotiate the curve coincides with that of the reference vehicle.

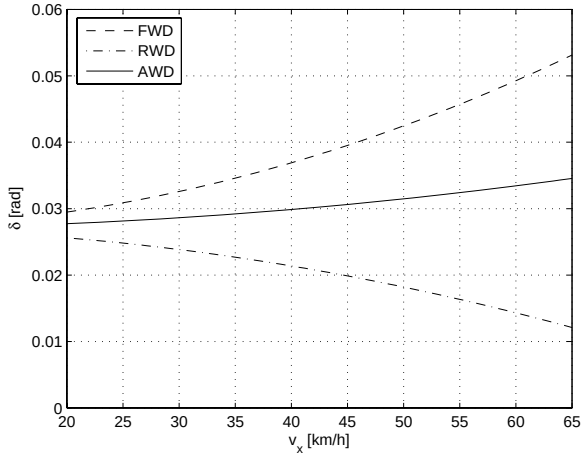

Figure 4. Steering angle δ required for various vehicle configurations to follow the same circular path.

For this maneuver the difference between the reference and actual yaw rate is plotted versus v_x and are shown in Figure (5).

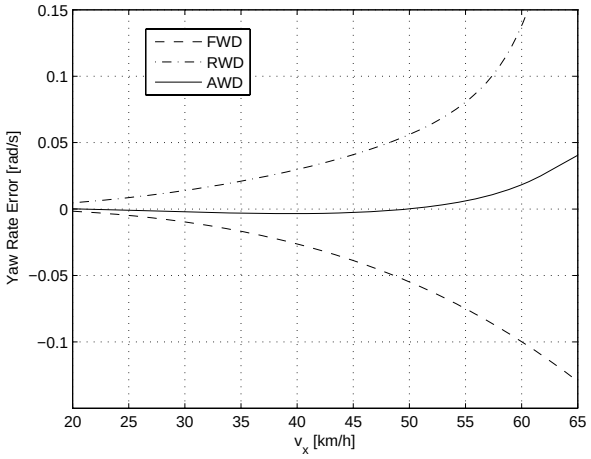

Figure 5. Yaw rate error ($\dot{\psi}^{\text{ref}} - \dot{\psi}$) for Constant Radius Turn

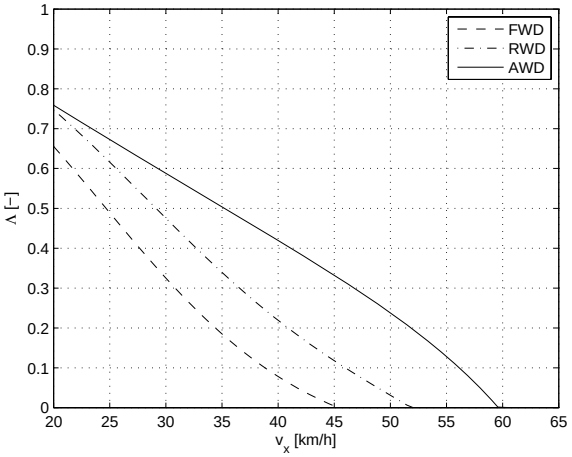

Figure 6. The vehicle safety margin (Λ) for Constant Radius Turn

The simulation results shown in (6) indicate that the vehicle safety margin Λ are essentially equal regardless of drive torque distribution, meaning it is a robust measure to detect a the safety limit The vehicle safety margin can now be used instead of the state errors to set the control boundaries between path-following control, driver warning and stability control (ESC). As an example the band between Λ = 1 → 0.3 could be used for path-following (state error elimination) using the AWD system, Λ = 0.3 → 0.2 for driver warning and Λ = 0.2 → 0 for stability control.

5. CONCLUSIONS

The paper shows how a vehicle safety margin relating a limit speed and the current speed and how this limit speed is defined. This proposed safety margin is independent of the yaw-rate error, commonly used as a reference for activating ESC systems. Additionally, the proposed safety margin is consistent regardless of longitudinal slip distribution. Future work should focus on an extension of the vehicle safety margin for dynamic maneuvers, i.e. when the vehicle is not in steady-state.

REFERENCES

[1] P. Borio et al. "Evaluation Criteria for AWD Vehicle sSystem Analysis". SAE 2004-01-2086 (P-386), (2004).

[2] Y. Ghoneim et al. "Integrated Chassis Control System to Enhance Vehicle Stability". International Journal of Vehicle Design 2000 - Vol. 23, No.1/2, (2000).

[3] R. Daily, D. M. Bevly and W. Travis. "Estimation of Critical Tire Parameters Using GPS Based Sideslip Measurements". SAE 2006-01-1965, (2006).

[4] M. Uchanski, S. Müller and K. Hedrick. "Estimation of the Maximum Tire-Road Friction Coefficient". Journal of Dynamic Systems, Measurement, and Control DECEMBER 2003, Vol. 125, (2002).

[5] H-P. Willumeit, et al."Mathematical models for the computation of vehicle dynamic behaviour during development". IMechE 925046, (1992).

[6] Y Yasuil. "Estimation of Lateral Grip Margin Based on Self-aligning Torque for Vehicle Dynamics Enhancement". SAE 2004-01-1070, (2004).

[7] E Ono, Y Hattori, Y Moragashi, and K Koibuchi. "Vehicle dynamics integrated control for four-wheel distributed steering and four-wheel-distributed traction/braking systems". Vehicle Taylor and Francis, System Dynamics, Vol. 44, No. 2, February 2006, (2006).

[8] ISO, editor. "Road Vehicles - Steady state circular test procedure". ISO 4138, (1991).

[9] H. Pacejka. "Tire and Vehicle Dynamics". Woburn, MA: Butterworth-HeineMann,ISBN 0-7680-1126-4, (2002).

APPENDICES

A. TIRE MODEL

The tire model used in this paper a modified version of the brush tire model, which has become increasingly popular in vehicle dynamics control and is well described in recent literature such as [9]. Longitudinal slip changes the lateral tire characteristics as can be seen in Figure (8). Excessive longitudinal slip on the front wheels, in a FWD vehicle will lead to final understeer and RWD vehicle oversteer as discussed in the introduction. For this reason a simple, but sufficiently comprehensive tire model is required. Assumptions

- Isotropic tire properties ($C_\kappa = C_\alpha = C$).
- Parabolic pressure distribution.
- Carcass deflections do only affect the dynamics of the tire.

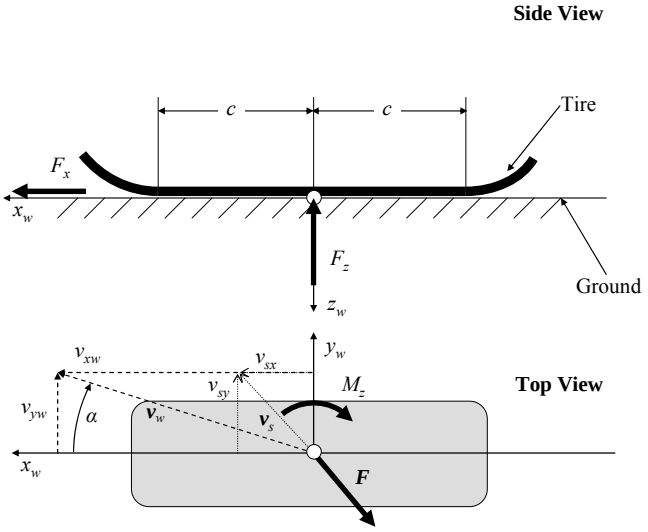

Figure.7. Tire nomenclature

A.1 Tire Inputs

Tire model inputs are the slip angle α ,the longitudinal slip κ and the normal load F_z. Given in wheel coordinates we have:

$$\tan(\alpha) = \frac{v_{sy}}{v_{xw}} \tag{17}$$

$$\kappa = -\frac{v_{sx}}{v_{xw}} \tag{18}$$

, using the definitions in Figure (7).
Tire model inputs are the lateral slip σ_y, longitudinal slip σ_x and the normal load F_z. The only required tire property is the rubber stiffness c_p given at a nominal contact patch length c_0 and normal load F_{z0}.

$$c = c_0\sqrt{\frac{F_z}{F_{z0}}} \tag{19}$$

$$C = 2c_p c^2 \tag{20}$$

$$\theta = \frac{C}{3\mu F_z} \tag{21}$$

$$\sigma_x = \frac{\kappa}{1+\kappa} \tag{22}$$

$$\sigma_y = \frac{\tan(\alpha)}{1+\kappa} \tag{23}$$

$$\sigma = \sqrt{\sigma_x^2 + \sigma_y^2} \tag{24}$$

$$\lambda = 1 - \theta\sigma \tag{25}$$

A.2. Tire Outputs

The total tire force is:

$$F = \begin{cases} \mu F_z(1-\lambda^3) & \text{if} \sigma \le 1/\theta \\ \mu F_z & \text{otherwise} \end{cases} \tag{26}$$

From which the longitudinal and lateral forces are now calculated as:

$$\begin{bmatrix} F_x \\ F_y \end{bmatrix} = F\frac{1}{\sigma}\begin{bmatrix} \sigma_x \\ \sigma_y \end{bmatrix} \tag{27}$$

The special case for wheel lock/spin ($|\kappa|$=1), the following formulas are used:

$$F_x = \mu F_z \cos(\alpha) \quad (28)$$

$$F_y = \mu F_z \sin(\alpha) \quad (29)$$

The self aligning torque is calculated from the pneumatic trail:

$$t = -c\frac{\lambda^3}{1+\lambda+\lambda^2} \quad (30)$$

$$M_z = tF_y \quad (31)$$

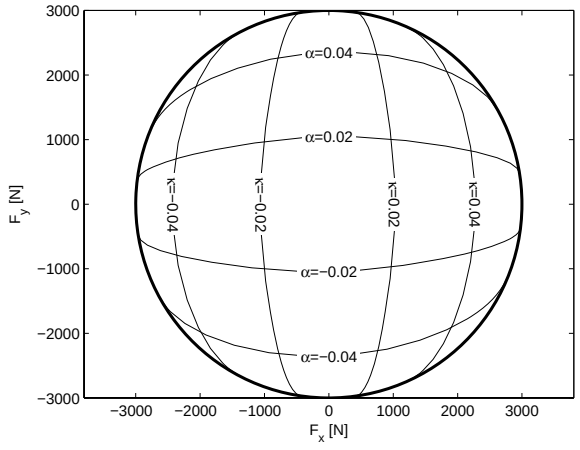

Figure 8. Combined Tire Slip @ constant levels of and α ($\mu = 1$, $F_z = 3$ kN and $\theta^{-1} = 0.15$)

The brush model in this form is supposed to describe the longitudinal tire behavior well. The lateral behavior is, as mentioned earlier, affected by the flexibility in the carcass which is neglected here.

A.3. Tire Linearization

If desired, the tire properties can be linearized in each point as follows:

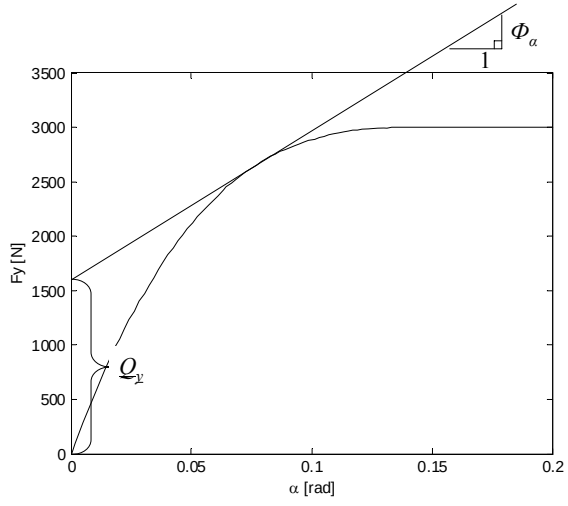

Figure9. Tire Linearization Parameters

$$F_y = \Phi_\alpha \tan(\alpha) \approx \Phi_\alpha \alpha \quad (32)$$

where,

$$\Phi_\alpha = \frac{\partial F_y}{\partial \sigma_y}\frac{1}{1+\kappa} = 3\mu F_z \frac{\sigma_y \theta \lambda^2}{\sigma(1+\kappa)} \quad (33)$$

A.4. Tire Dynamics

Tire force build-up delay caused by carcass deflections is handled by the use of a simple first order dynamic filter, where the time-constant is vehicle speed dependent.

$$F_i = \frac{1}{1+\tau_i s}F_i^{ss} \quad (34)$$

$$\tau_i = \frac{3L_i}{v_x} \quad (35)$$

Where s is the Laplace operator, $i=r,f$ and L_i the relaxation length, which is the rolled distance of the tire until the carcass deflections are built up to sustain the tire forces.

B. VEHICLE DATA

The vehicle used in the simulations is a typical mid-size passenger vehicle which data is listed below.

B.1. Vehicle Parameters

Parameter	Unit	Description
m = 1675	[kg]	Curb weight
I = 2617	[kg m^2]	Total z-moment of inertia.
h = 0.5	[m]	Height of CoG above ground.
L = 2.675	[m]	Wheel base
a = 0.4L	[m]	Distance from CoG to front axle
b = L - a	[m]	Distance from CoG to rear axle
μ = 0.4	[-]	Road friction
A_f =2.17	[m^2]	Frontal area
C_d = 0.30	[-]	Air drag coefficient

Table B.1 Vehicle Parameters

B.2. Tire Data

The tire used in the simulations is a general 205/60R14 tire, measured at μ=0.87 In order to capture the non-linear load-dependency found when measuring the tire, the cornering stiffness was re-written by curve-fitting tire data using a second-order polynomial.

c_1 = -0.0012	c_2 = 19	c_3 = 9500
$d_1 = -6.6\cdot10^{-5}$	d_2 = 1.3	d_3 = −210

Table B.2 Tire Parameters

The cornering stiffness C_α now becomes:

$$C_\alpha = c_1 F_z^2 + c_2 F_z + c_3 \quad (36)$$

Similarly the peak lateral force D is defined as:

$$D = d_1 F_z^2 + d_2 F_z + d_3 \quad (37)$$

The normal force in the brush model F_z can now be replaced with the tire-data based pseudo-normal force D.

Parameter	Unit	Description
L_x = 0.022	[m]	Long. tire relaxation length
L_y = 0.565	[m]	Lateral tire relaxation length

Table B.3 Tire Dynamics